CHARACTERISTIC LENGTHS AFFECTING EVAPORATION FROM HETEROGENEOUS POROUS MEDIA WITH SHARP TEXTURAL BOUNDARIES

D. Or, P. Lehmann, N. Shokri

Soil and Environmental Physics Laboratory (LASEP); School of Architectural, Civil and Environmental Engineering (ENAC); Ecole Polytechnique Federale de Lausanne (EPFL); Lausanne, Switzerland

ABSTRACT. The propagation of evaporation drying front into initially saturated porous medium results from capillary-driven liquid flow from large pores at the front supplying evaporation from smaller pores at the surface. Similar to other displacement processes, the drying front may exhibit irregular spatial patterns due to pore size variations. In heterogeneous media containing sharp textural contrasts, drying front displacement may follow preferential path corresponding to liquid flow from coarse textured regions in support of evaporation from saturated fine textured regions connected to the surface. Hele-Shaw cells with vertical and horizontal sharp textural interfaces between coarse and fine sand domains were used to study water distribution during evaporation using neutron transmission technique and imagery with dyed water. For vertical textural interfaces, evaporation from saturated fine sand was sustained by liquid flow from adjacent coarse sand resulting in preferential advance of the drying front exclusively into coarse sand region. Direct evidence of water flow pathways from coarse to fine sand was obtained with neutron radiography using heavy water as a tracer. A characteristic length defining maximum drying front depth (in the coarse medium before air enters the fine sand) is determined by the difference in air-entry values of the two media. In our experiments, viscous resistance exerted no effect on maximum front depth even when flow cross section (fine sand relative area) was reduced from 75% to 8% under similar external evaporative conditions (viscous limitations were not important here). For horizontal layers of fine over coarse sand, the drying front initially propagates in fine sand until air first enters the coarse sand resulting in an abrupt and disproportionally large displacement of water from coarse to overlaying fine layer driven by capillary pressure difference between air entry values of the sands. Subsequent to rapid pressure relaxation, drying front invades preferentially the coarse layer with no changes in liquid distribution in the overlaying fine layer. Experiments with layers of different thicknesses and positions (depths) relative to evaporative surface revealed the importance of other characteristic length spanned by pore size distribution of the medium. The combination of intrinsic capillary characteristic length and the position of a textural interface below the surface defines the ultimate depth of drying front in layered media (hence magnitude of evaporative losses). Preferential evaporation patterns from texturally-heterogeneous media during capillary driven liquid flow result in an increase in overall evaporative losses relative to porous media represented by homogenous effective properties.

1.- Introduction

The drying of soils and other porous media is characterized by formation and motion of a drying front separating the liquid saturated and unsaturated domains. The motion of the drying front is a result of invasion of gaseous phase replacing evaporating liquid. Evaporation is a key process for water exchange between soil and atmosphere; it is involved in plant physiological function through transpiration, and affects the amount of available water for plants and microorganisms inhabiting the soil. Drying processes are of significant industrial and engineering importance including food processing and preservation, production of ceramics and paper, and numerous construction activities. Notwithstanding the prominent role of drying in many applications, prediction of drying rates from porous media remains a challenge. Evaporation rate is affected by both atmospheric demand (humidity, temperature and velocity of ambient air), and by porous medium pore space and transport properties (thermal and hydraulic conductivities and vapor diffusion). Consequently, complex and highly dynamic interactions between media properties, transport processes, and boundary conditions result in wide range of evaporation behaviors.

Considering effects of soil properties and heterogeneity on evaporation behavior, we scale actual evaporation rate e by potential evaporation rate e_0 occurring under similar conditions from a free water surface. The relative drying rate (e/e_0) from an initially saturated porous medium exhibits distinctly different stages used for diagnostics of transport mechanisms, and interpretation of the rate limiting processes. Typically, a 'constant rate period' equal to the potential rate occurs until surface water content or drying front depth reach certain critical values. Subsequently, the drying rate decreases significantly as evaporation becomes limited by vapor diffusion through the porous medium. In the following text the period not limited by liquid flow to the evaporating surface is denoted as stage-1. Due to the resistance of a viscous air boundary layer at the surface the drying rate may be reduced during stage-1 as discussed in Shokri et al. (2007, Water Resources Research, under review).

Changes in drying rates are linked with liquid distribution within the porous medium and with internal transport mechanisms. Many studies have shown that high evaporation rates sustained even during penetration of a drying front into the porous medium are associated with continuous water films connecting the drying front with evaporating surface (Yiotis et al., 2004). The key questions are (1) what conditions support formation and sustain a continuous liquid network between evaporating surface and drying front? and (2) what characteristics promote formation of capillary gradients that induce sufficient flow to supply water evaporating at the surface?

Some of these issues were addressed in a recent study by Lehmann et al. (2007, *Characteristic lengths affecting evaporative drying from porous media, Phys. Rev. E., under review*) focusing on resolving important characteristic lengths and linking evaporation behavior with porous media characteristics for uniform media. Some of the key results from Lehmann et al. (2007) will be highlighted to enable extension of the results to heterogeneous porous media, considering, as a first step, simple heterogeneities such as abrupt textural changes. The specific objectives are to quantify effects of textural discontinuities on (1) drying front patterns, (2) duration of stage-1 evaporation, and (3) total evaporative water losses as compared with homogeneous porous medium under similar conditions.

2.- Theoretical considerations

2.1. Capillary-driven evaporative flows and characteristic lengths

Scherer (1995) and others have shown that the spatial extent of (capillary) flow-supporting film region depends on (i) characteristics of the porous medium that generate the driving capillary force gradient between water-filled fine pores at the surface and large pores at the front, (ii) drying front depth, and (iii) viscous resistance to flow through liquid films. Typically, the capillary pressure gradient towards the surface is opposed by gravitational forces and viscous dissipation. Lehmann et al. (2007) have shown that the spatial extent of the film region is a function of pore size distribution and can be deduced from soil type and other simple textural and water retention information.

For simplicity, we represent a vertical textural boundary between coarse and fine-textured domains within a porous medium as a pair of hydraulically-connected capillaries (see inset Fig. 1. Both capillaries are initially liquid-filled, and as liquid evaporates, capillary menisci form and result in capillary pressure (head) drop *h.* The largest capillary pressure attainable within the large capillary with radius r_2 (representing a coarse-textured domain) is defined by its air-entry value $h_b(r_2)$. Subsequent evaporation from the system would not change meniscus curvature within the large capillary and a capillary pressure difference forms between the large and small capillary which may attain a higher curvature. Consequently, water flows from the large to the small capillary resulting in a receding meniscus in the large capillary. As evaporation progresses, the distance to the evaporating surface increases until the air entry value in the small capillary with radius r_2 is reached. Thus, the maximum capillary drive L_{cap} expressed in units of length for the two capillaries is given as:

$$L_{cap} = \frac{2\,\sigma}{\rho\,g}\left(\frac{1}{r_1} - \frac{1}{r_2}\right) \tag{1}$$

with g, acceleration due to gravity, σ, surface tension and ρ, water density. This is the length at which gravitational head balances the maximum capillary driving force causing cessation of flow, and could also be viewed as characteristic gravity length (L_G), L_G=L_{cap} for the pair of vertical capillaries considered.

For high evaporation rates in fine capillaries, liquid flow may involve significant viscous dissipation with head loss proportional to flow velocity. The drying rate e_0 from a pair (or more) capillaries with total cross-sectional area A is supplied by flux density q flowing through the fine capillary (r_1):

$$e_0\,A = q\,\pi\,r_1^2 \rightarrow q = e_0\left(1 + \frac{r_2^2}{r_1^2}\right) \tag{2}$$

Evaporation from the meniscus in the small capillary is supplied by liquid flow according to Poiseuille’s equation:

$$e_0\left(1 + \frac{r_2^2}{r_1^2}\right) = q = \frac{\pi\,r_1^2\,\rho\,g}{8\eta}\frac{\Delta h}{L} \tag{3}$$

with the height difference between the large and small menisci L, q water flux density in the small capillary, and η dynamic viscosity, the factor 8 for cylindrical capillary shape and the pressure drop due to viscous dissipation Δh. To quantify the characteristic length associated with viscous dissipation (L_V) it is instructive to consider horizontally oriented pair of capillaries (no gravity). The maximum distance between menisci such that viscous dissipation balances capillary driving force, L_V, is given as:

$$\frac{2\sigma}{g\rho}\left(\frac{1}{r_1}-\frac{1}{r_2}\right)=\frac{8L_v\,e_0\,\eta\left(r_1^2+r_2^2\right)}{\rho\,g\,\pi\,r_1^4}\rightarrow L_V=\frac{\rho\,g\,\pi\,r_1^4}{8\,e_0\,\eta\left(r_1^2+r_2^2\right)}L_G \tag{4}$$

finally, considering combined effects of gravity and viscous dissipation for evaporation from a vertical pair of capillaries, the total (combined) distance L_C between menisci or maximum drying front depth is:

$$L_C=\frac{\dfrac{2\sigma}{g\rho}\left(\dfrac{1}{r_1}-\dfrac{1}{r_2}\right)}{\dfrac{8e_0\,\eta\left(r_1^2+r_2^2\right)}{\rho\,g\,\pi\,r_1^4}}\rightarrow L_C=\frac{L_G}{\left(1+\dfrac{L_G}{L_V}\right)} \tag{5}$$

as long as the gravitational length L_G is much shorter than the length defined by the viscous dissipation L_V, the combined length $L_C \approx L_G$.

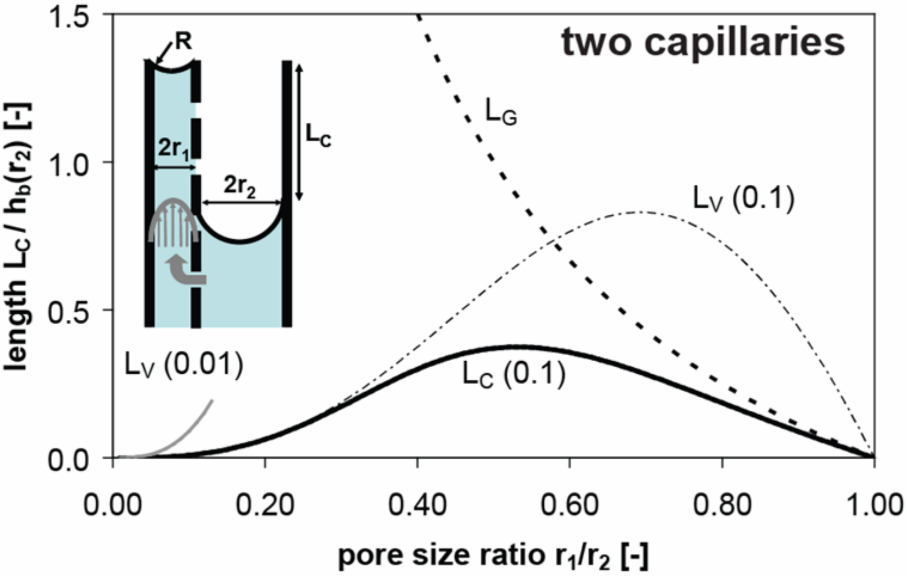

Fig. 1: The relative characteristic length L_C (scaled by r_2 air-entry value) marking the end of stage-1 evaporation from a pair of hydraulically-connected capillaries for two evaporation rates (indicated in parentheses as ratio between potential evaporation rate e_0 and conductance K_s of the pair of capillaries). Water flows from the receding meniscus in the large capillary r_2 (similar to motion of a drying front) to supply evaporation surface at the top of the fine capillary r_1. The characteristic length is the maximum front depth reflecting interplay between capillarity, gravity and viscous dissipation. Without viscous effects (L_V), the characteristic length (L_C) increases with decreasing pore size ratio r_1/r_2 reflecting increase in capillary driving force. The viscous dissipation length L_V decreases with enhanced drying rate.

The results above could be generalized by expressing the effect of the pore size difference (determined by r_2 and r_1) on evaporation characteristic lengths. The maximum distance between the surface and receding meniscus is shown as a function of r_1/r_2 in Fig. 1. For a small ratio ($r_1 << r_2$) the capillary forces are large supporting capillary flows for extended L_C. In contrast, for small ratio r_1/r_2, viscous flow through the fine capillary becomes limiting and the characteristic length L_C is shorter than the length determined by the interplay between capillary and gravitational forces alone. While the length L_G does not depend on the evaporation rate, L_V decreases with increasing e_0 due to the increased viscous losses. The characteristic lengths for viscous dissipation are shown for a drying rates e_0/K_s=0.1 and 0.01 with the conductivity of the pairs of capillaries K_s. The analyses above are easily extended to multiple hydraulically coupled capillaries, or to soils with known pore size distribution as shown in Lehmann et al. (2007).

2.2. Evaporation from porous media with sharp textural contrasts

A relatively simple extension of the results for hydraulically-interaction pair of vertical capillaries is possible for evaporation from porous media containing abrupt textural boundaries separating domains with well-segregated pore sizes. For vertically-oriented textural boundaries such as shown in the Hele-Shaw cell in Fig. 2c the depth of the maximum drying front in the coarse sand before air enters the fine can be approximated from the difference in the respective air entry values for the two materials as we'll show in subsequent experimental results. This simple extension of the results from the pair of capillaries implies additional significant differences compared to the homogeneous porous medium case, for example the overall water losses are generally larger than losses from homogeneous columns of either porous medium (Figs. 2a and 2b), and the drying patterns are preferential reflecting capillary-induced liquid flow from coarse to fine domains (Fig. 2c). For horizontal textural contrasts (layers), the thickness of the layers and the sequence of layering plays important role in the resulting extent and pattern of drying. When the first tip of the drying front reaches the boundary in an arrangement of fine over coarse layers, air invading the coarse material results in a cavitation-like pressure relaxation and rapid and intense water flow from the coarse to the fine layer. When the fine layer thickness is less than its characteristic length evaporation takes place subsequently from a stationary wet surface within the fine layer as water is supplied from coarse domain via mass flow as seen in Fig. 2d. Other horizontal arrangements that capitalize on additivity or interference of characteristic are analyzed in an actual series of laboratory experiments.

3.- Experimental Setup

3.1. Evaporation from Hele-Shaw cells

Evaporation rates from glass Hele-Shaw cells (250 mm in height, 73 mm in width and 10 mm thickness) filled with segregated domains of sands with contrasting particle sizes in the range of 0.1-0.5 mm (denoted as "fine") and 0.3-0.9 mm ("coarse") were measured. Each cell was initially saturated and placed on a digital balance to measure mass loss (evaporation rate) at 60 s intervals. The atmospheric demand was monitored by measuring potential evaporation rate from free water surface, as well as temperature and relative humidity of the air. In most experiments we used water dyed with brilliant blue to enhance contrast between saturated and dry (evaporated) zones as seen in Fig. 2.

3.2. Neutron radiography measurement

For some experiments we used neutron transmission radiography at the Spallation Neutron Source of the Paul Scherrer Institute (PSI), Villigen, Switzerland (Lehmann et al., 1999). Neutron transmission radiographs were obtained every 5 minutes with a scanning time of 12 seconds per image covering 100x100 mm field of view. Radiographs were recorded with a Peltier cooled (-45 deg Celsius) slow scan CCD camera featuring a 1024x1024 pixel chip with an effective spatial resolution of 0.1 mm and a dynamic range of 24'000 gray levels. For these experiments we used a Hele-Shaw cell filled with sand differing in particle sizes occupying side by side domains. To enhance traceability of water exchange between the domains we used heavy water to saturate the column to a depth of 60 mm below the surface topped with dyed (normal) water. Mass loss rates during evaporation were monitored by digital balance as well as deduced from image analyses of neutron radiographs (Shokri et al., 2007).

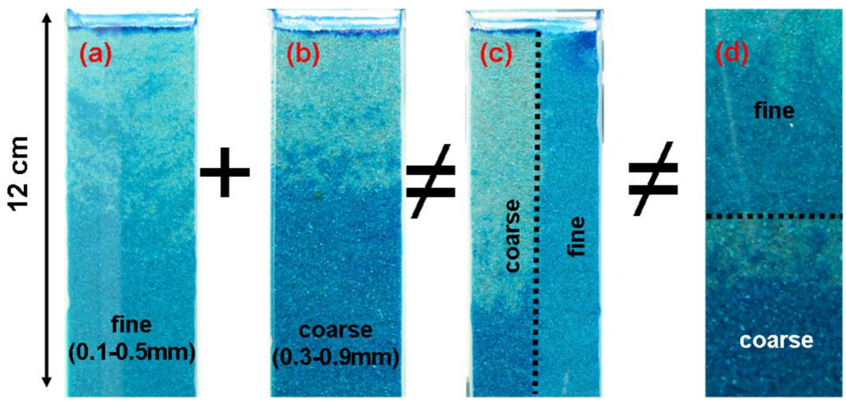

Fig. 2: Drying experiment with Hele-Shaw cells subjected to similar boundary conditions. Dark blue zones correspond to water filled regions. For homogeneous sand (a, b) the drying rates are similar but more wet structures are left above the drying front in the fine sand. When two sands are interacting through a vertical interface (c), water flows from the coarse to the evaporating surface of the fine. In case of a horizontal interface, a partially air-filled zone in the coarse below the wet fine zone forms (d).

4.- Results and Discussion

4.1. Evaporation patterns from Hele-Shaw cells with vertical textural contrast

In the presence of sharp vertical textural contrast the evaporative drying front propagates preferentially into the coarse sand region while fine sand domain remains fully saturated. This preferential drying pattern reflects capillary driven flow from coarse to fine region to supply water evaporating from top (of the saturated fine region) surface. Evaporation patterns just before the air phase enters the fine material are shown in Fig. 3 (bottom) for Hele-Shaw cells filled with different proportions of fine domain (expressed as percent fine). A striking feature unifying all these experiments is the remarkably consistent depth of drying front about 10 cm irrespective of the fraction of fine domain in the Hele-Shaw cell. The constant depth of drying front should not be confused with mass loss, as the amount of mass lost for the same drying front depth in the coarse is proportional to the fraction of the coarse domain (serving as the supply region for sustaining evaporation). As discussed in the theoretical section of this study, the maximum drying front before air enters the fine sand is attributed to the capillary driving force between the textural domains where the characteristic length is simply the difference in air entry values for the two sands. These front depths are in agreement with characteristic length deduced from the respective water retention curves depicted in Fig. 3 (top).

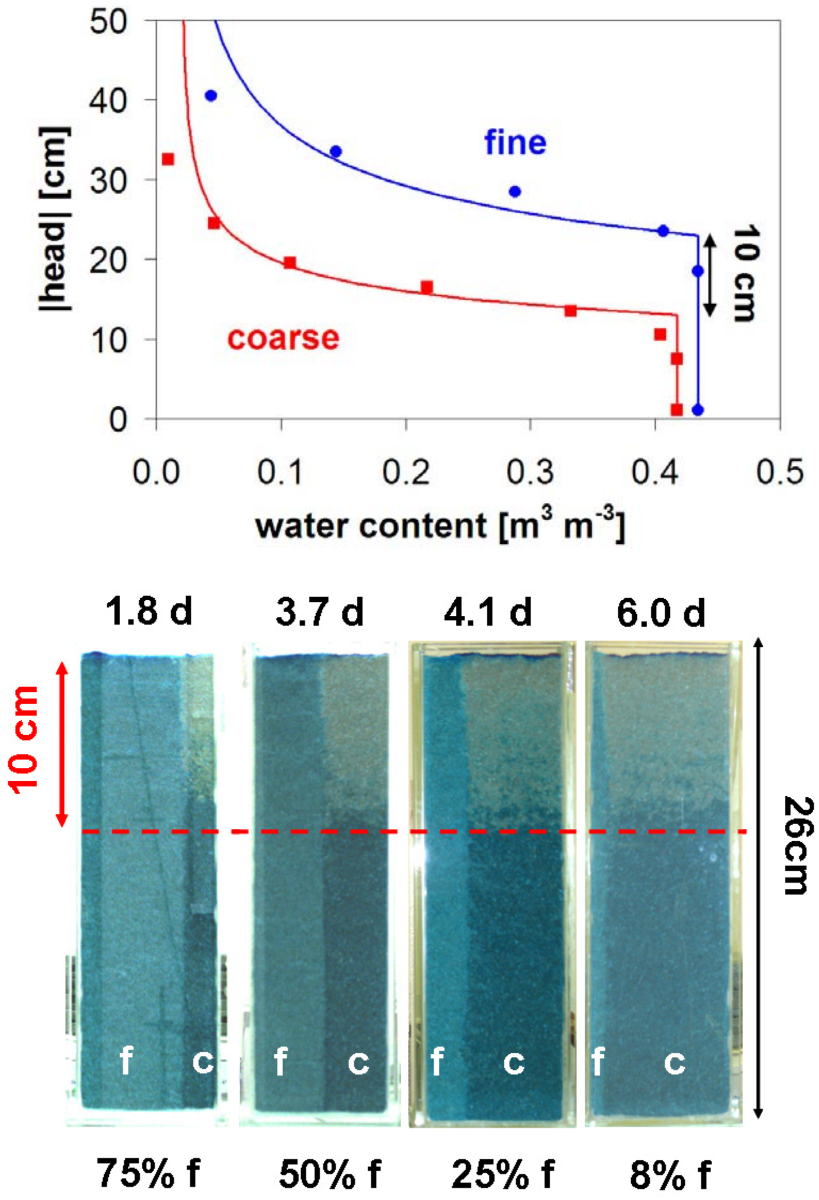

Fig. 3: Water retention curve (top) and dye distribution just before the entrance of air in the fine sand (bottom). The depth of the drying front in the coarse (**c**) sand is roughly the difference in the air-entry values of the two materials. The numbers above the cells in the bottom figure indicate the time of the experiment in days. The percentage of the fine (**f**) sand is added below the figure.

Another important observation deduced from this series of experiments is the relatively constant evaporation rate from Hele-Shaw cells containing a range of fine sand fraction that was sustained for longer periods than stage-1 evaporation for homogeneous Hele-Shaw cells containing either coarse or fine sand only (Fig. 4). In other words, whether the fine sand fraction is 75% or 8% the evaporation rate remained rather constant and overall evaporation (mass loss) was higher in heterogeneous cells. These results also suggest that viscous limitations to flow through the fine sand were not significant in these experiments. These are expected to play more prominent role when the fine domain in composed of clay fraction or similar porous media.

4.2. Neutron radiography measurement of lateral flow between vertical domains

The series of experiments with heavy water as a tracer and observed drying patterns using neutron radiography imaging yielded conclusive evidence regarding the mechanisms, patterns, and rates of internal exchanges due to capillary flows between the fine and coarse domains as depicted in Fig. 5

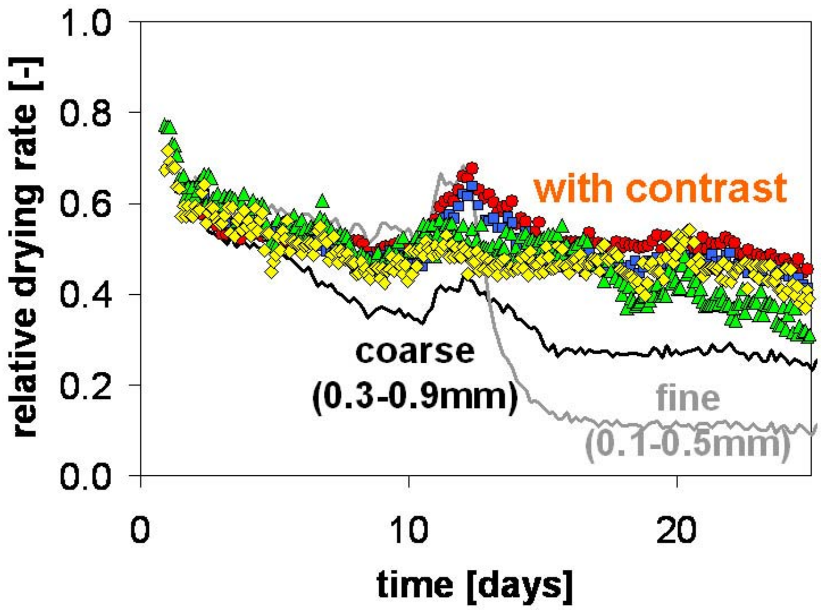

Fig. 4: Relative evaporation rate of two homogeneous columns and four "textural contrast" cells (from Fig. 3 above) with different cross-sectional fractions of fine and coarse domains. Relative to losses from the homogeneous columns, the drying rate in cells with vertical textural interface remains higher and is virtually independent of the fine sand fraction (indicating no viscous limitations by hydraulic conductivity).

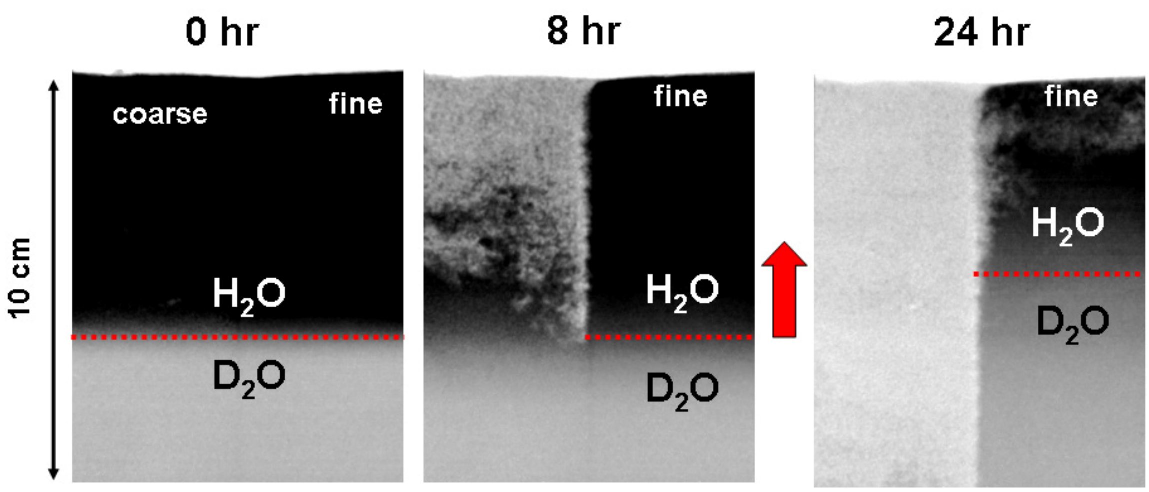

Fig. 5: Neutron transmission images of a Hele-Shaw cell with a vertical contrast filled with heavy (D_2O) and light water (H_2O). First, the drying front enters the coarse part and the coarse sand supplies evaporation from the surface of the fine textured material. This water flow can be visualized by the rising interface between heavy and light water (dashed red line). Heavy water flows from the coarse towards the surface of the fine sand.

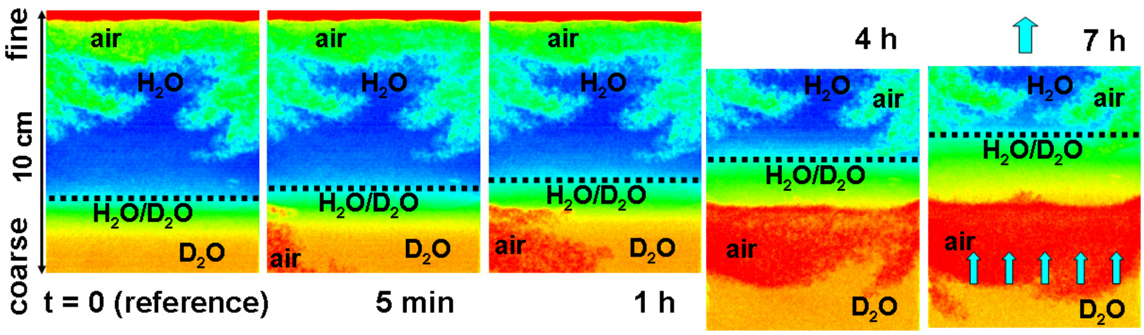

Fig. 6: Invasion of air in the coarse sand below a layer of fine sand analyzed using neutron radiography. Due to pressure relaxation, water is pushed upwards from the coarse to the fine sand. A drying front develops in the coarse sand and heavy water moves from the coarse to the fine sand to replace water evaporated from the surface.

The experimental results in Figure 5 show upward motion of the interface between the heavy and regular water. Heavy water from the receding drying front in the coarse flows to the fine textured surface. The fine sand remains saturated until the drying front depth in the coarse part was about 10 cm corresponding to the characteristic length defined by the differences in air entry values.

4.3. Evaporation patterns from horizontally layered textural contrast

The more ubiquitous scenario of near surface layering (due to soil profile development, surface crust, or mulch) provides some insights regarding the abrupt changes taking place when evaporation drying front crosses the horizontal textural interface. The images shown in Fig. 6 were obtained in another series of neutron radiography experiments. The behavior was similar to that already observed in Fig. 2d with dyed water. For initially H_2O-saturated fine over D_2O-saturated coarse sand layers the drying front traverses the fine layer in a similar fashion as through uniform sand column. However, as soon as the tip of the evaporative drying front penetrates the coarse sand a rapid and disproportionate water displacement from the coarse to the fine sand takes place. The pressure in the coarse part changes abruptly from its air-entry value to the air-entry value at the front related to the fine sand. The air-entry value associated with the fine sand corresponds to a dry state of the coarse material and a large volume of liquid is released rather quickly. Pressure equilibrates when sufficient water is displaced and viscously dissipating the excess energy. The use of heavy water interface enabled direct observation (and quantification) of this pressure equilibrium process as indicated by upwards moving front D_2O/H_2O in the fine sand in Fig. 6 (7h). Heavy water flows from the drying front in the coarse to supply water evaporating from the surface.

Additional experiments with different combinations of layer thickness and sequences of layering are subjects of ongoing studies.

5.- Summary and Conclusions

The study extended the concept of characteristic lengths that control stage-1 evaporation from soils and other porous media. The notion that stage-1 evaporation is supported by capillary (liquid) flows is extended to heterogeneous media with abrupt textural boundaries. For vertical textural boundary, drying takes place preferentially in the coarse domain to supply evaporation from the saturated fine textured domain. The maximum drying front depth within the coarse sand (while fine sand remains completely water saturated) corresponds to the difference in the air-entry values of the two media. Irrespective of the fraction of fine sand in the domain, we observed prolonged stage-one evaporation resulting in more water loss in the heterogeneous system (even when fine sand fraction was 8%) than would be expected in homogeneous (or homogenized) system under similar conditions.

Direct evidence for capillary flows and displacement patterns were obtained with neutron radiography measurements where heavy water was used a tracer. We observed drying front preferential displacement in coarse sand region while fine sand region remains fully saturated. The upward motion of the heavy/normal water interface provided direct evidence of the capillary-induced flows from the drying front to the surface. Neutron radiography experiments were also instrumental in clarifying the abrupt displacement processes when drying front crosses fine over coarse interface. The rapid displacement and pressure equilibration were followed by an additive capillary-induced evaporation process where the front propagates preferentially in the coarse layer while the front in the fine layer remains stationary.

This study highlights the role of heterogeneity in enhancing soil evaporation relative to homogeneous soils. The findings provide predictive capabilities and more realistic assessment of soil evaporation, and may provide a means for controlling evaporation by proper selection of materials with prescribed characteristic lengths and layering patterns.

Acknowledgements: This project (2000021-113676/1) is funded by the Swiss National Science Foundation. The authors gratefully acknowledge the assistance of Peter Vontobel and the NEUTRA team at PSI.

References

Lehmann, E. H., P. Vontobel, P., and L. Wiezel, Proc. 6th World Conf. on Neutron Radiography, Osaka, 151–158, 1999

Lehmann, P., S. Assouline, and D. Or, Phys. Rev. E (in review), 2007

Scherer G.W., and D.M. Smith, Journal of the Non-Crystalline Solids 189, 197–211, 1995

Shokri, N., P. Lehmann, P. Vontobel, and D. Or, Water Resour. Res. (in review), 2007

Yiotis, A.G., A.G. Boudouvis, A.K. Stubos, I.N. Tsimpanogiannis, and Y.C. Yortsos, AIChE J., 50, 2721–2737, 2004